



# The Influence of the Madden–Julian Oscillation on the Wet Season Rainfall over Saudi Arabia

Mansour Almazroui<sup>1,2</sup>

Received: 5 May 2022 / Revised: 14 November 2022 / Accepted: 17 November 2022  
© The Author(s) 2022

## Abstract

The influence of Madden–Julian oscillation (MJO) is examined on intraseasonal rainfall variability during the wet season (November–April) by using the real-time multivariate (RMM) MJO index, ERA5 reanalysis, and daily observed rainfall dataset from 26 stations in Saudi Arabia for the period 1985–2021. The MJO 8 phases are categorized into wet (phases 1, 2, 7 and 8) and dry (phases 3, 4, 5, and 6) based on the Saudi Arabian intraseasonal rainfall characteristics associated with MJO phases. It is observed that 41% (46%) of total (extreme) rainfall events occur during the MJO wet phases, while only 23% (18%) of such events occur during MJO dry phases. The intraseasonal variability signals are isolated from daily dataset by applying a 30- to 90-day period bandpass filter. The analyses are validated by constructing composites of daily filtered precipitation anomalies during MJO 8 phases. The physical mechanism indicates that the significant intraseasonal wetter conditions are linked with enhanced easterly and southeasterly moisture convergence over Saudi Arabia from the Arabian Sea. The atmospheric cyclonic circulation anomalies during the wet phases favor more moisture convergence and vertical moisture advection, which may lead to enhanced convection and rainfall. However, during the dry phases, anticyclonic circulation anomalies enhance moisture divergence and reduce vertical moisture advection and consequently suppress the convection and rainfall activity over Saudi Arabia. The analyses show that the intraseasonal rainfall variability over Saudi Arabia is significantly influenced by the MJO during the wet season. These findings have important implications for sub-seasonal rainfall forecasting in Saudi Arabia.

**Keywords** Madden–Julian oscillation · Wet season · Intraseasonal rainfall · Moisture convergence · Moist static energy · Saudi Arabia

## 1 Introduction

Precipitation is an important, but complex climate system component that requires accurate understanding for risk management. Therefore, knowing the influence of large-scale circulation patterns that govern precipitation generating systems is essential for managing water resources, agriculture, reducing the risk of drought and flash flood hazards in a region. The Arabian Peninsula is a semi-arid to arid climatic region where annual rainfall is relatively low

compared to other northern hemispheric regions (Almazroui et al. 2020). Mainly, the rainfall occurs from November to April, known as the wet season (Abid et al. 2016). During the wet season, the region experiences extreme rainfall events (De Vries et al. 2018), leading to natural hazards, particularly in Saudi Arabia. The vulnerability of arid and semi-arid regions to flash floods has been shown to be equal to that of areas with heavy rainfall events (Zipser et al. 2006; Haggag and El-Badry 2013; Tippett et al. 2015). For example, in January 2005 and 2011, and in November 2009, Saudi Arabia experienced heavy rainstorms and flash flood events which caused massive loss to infrastructure and human casualties (Almazroui 2020; De Vries et al. 2016; Yesubabu et al. 2016). Therefore, it is pertinent to understand the intraseasonal variability of Saudi Arabian wet season rainfall, which may be modulated by the Madden–Julian oscillation (MJO). This is the main focus of the current research work.

✉ Mansour Almazroui  
mansour@kau.edu.sa

<sup>1</sup> Center of Excellence for Climate Change Research/  
Department of Meteorology, King Abdulaziz University, P.  
O. Box 80234, Jeddah 21589, Saudi Arabia

<sup>2</sup> Climatic Research Unit, School of Environmental Sciences,  
University of East Anglia, Norwich, UK

Saudi Arabia extends in latitude from the tropical to the subtropical region, surrounded by the water bodies like the Red Sea in the west, the Arabian Gulf in the east, and the Arabian Sea to the south. The seasonal rainfall variability of Saudi Arabia is mainly modulated by the El-Niño Southern Oscillation (ENSO) phenomenon (Kang et al. 2015; Kamil et al. 2017; Abid et al. 2016; 2018; Ehsan et al. 2017). ENSO has significantly impacted interannual rainfall variability over the Arabian Peninsula since the mid-1980s due to the strengthening relationship between ENSO and regional rainfall (Kang et al. 2015). ENSO tends to provide the background state for the seasonal mean and may consequently lead to an increase in the interannual rainfall variability in the region.

Saeed and Almazroui (2019) found that mid-latitude circumglobal wave train (CGT) plays significant role on interannual precipitation variabilities in Saudi Arabia through Mediterranean disturbances during winter season. They found that CGT wave-like pattern is associated with upper air anomalous circulations over the region which is associated with the spatial precipitation distributions. The Mediterranean storms influence the intraseasonal (Tippett et al. 2015; Guo et al. 2017) and interannual (Almazroui et al. 2015; Kamil et al. 2017) rainfall variabilities in the Middle East. The frequency and intensity of Mediterranean disturbances are influenced by North Atlantic Oscillations (NAO) at interannual and intraseasonal timescales (Flaounas et al. 2022). The trajectories of North Atlantic storm tracks over Euro-Mediterranean region and NAO are closely related, such that NAO positive phases shift the Atlantic storm tracks toward north Europe, while NAO negative phases causing more Atlantic storm tracks over the Mediterranean region (Raible 2007; Pinto et al. 2009). The MJO events have significant influence on NAO phases (Cassou 2008), which consequently affect the storm trajectories over Euro-Mediterranean region. The anomalous Mediterranean cyclonic (anticyclonic) circulations associated with NAO impacts the winter season rainfall and temperature over Arabian Peninsula (Saeed et al. 2019, 2022). Further, MJO is also affected by the interannual variability associated with MJO and ENSO (Wilson et al. 2013; Sreekala et al. 2018).

MJO is another coupled ocean–atmospheric phenomenon on the intraseasonal time scale, contributing significantly to the weather extremes in different parts of the globe (Zhang 2005; Wu et al. 2016; Schwartz and Garfinkel 2017). The typical time scale of the MJO is between 30 and 90 days, and it has different phases from the Indian Ocean to the Pacific and Atlantic Oceans (Madden and Julian, 1994; Zhang 2005; Tian et al. 2011). The MJO is the large-scale atmospheric circulation mode of intraseasonal variability in the tropics (Madden and Julian, 1971, 1972; Zhang, 2005). The MJO modulates weather regimes at a synoptic scale in the tropics and extratropical regions such as North America (Whitaker

and Weickmann, 2001), North Atlantic Ocean (Han et al. 2008; Cassou, 2008), Africa (Pohl and Camberlin 2006; Alaka and Maloney 2012) and Asia (Jia et al. 2011; Pai et al. 2011). The wintertime (November to April) intraseasonal rainfall variability over southwestern Asia is modulated by MJO activity in the eastern Indian Ocean (Barlow et al. 2005). Some studies also suggest that MJO influences the interannual variability of precipitation (Hendon et al. 1999; Slingo et al. 1999). However, very few studies have investigated its impact on the rainfall and associated mechanism over the Arabian Peninsula region.

Nazemosadat and Ghaedamini (2010) explored the MJO impact on daily, monthly, and seasonal precipitation over southern Iran and the Arabian Peninsula and categorized the MJO events into two combinations, with phases 1, 2, 7, and 8 as negative and phases 3, 4, 5 and 6 as positive. The negative MJO phases favor moisture advection from the Arabian Sea into southern Iran and the Arabian Peninsula, bringing wetter and occasionally more extreme weather conditions to the region. Meanwhile, positive MJO phases are associated with dry conditions due to the advection of dry air from the north (Pourasghar et al. 2015). Furthermore, the intraseasonal rainfall predictability is significantly modulated by MJO, and this shows that weather extremes may be predictable if we increase the understanding of the MJO relationship with the regional rainfall (Vigaud et al. 2019; Merryfield et al. 2020). Therefore, MJO potentially plays a vital role in influencing intraseasonal climate variability, which can link directly with weather forecasting and be used as an indicator precursor for extended-range forecasting (Zhang et al. 2013; Tippett et al. 2015).

In the current study, observed daily station dataset is used to pinpoint which MJO phases bring wetter and drier conditions to Saudi Arabia. The dynamic and the thermodynamic mechanisms which may be helpful in the correct forecasting of extreme weather events were discussed in detail. In this study, the influence of MJO 8 phases on intraseasonal rainfall variability in Saudi Arabia was investigated. The data and the methods are discussed in Sect. 2. The influence of MJO on Saudi Arabian wet season rainfall events and the underlying physical mechanism are discussed in Sect. 3. The summary and conclusions are discussed in Sect. 4.

## 2 Data and Methodology

### i. Data

In this study, the daily observational rainfall dataset was obtained from 26 stations across Saudi Arabia, spanning the domain (18–31° N; 39–50° E) for the period 1985–2021 (Almazroui 2011). This observational rainfall record was obtained from the Saudi Arabia National Center for Meteorology (NCM). Using this station rainfall dataset,

the frequency of wet season rainfall events was calculated during the period 1985–2021. The frequency of extreme rainfall events was also calculated using the methodology adopted by Almazroui (2020). Extreme rainfall events are defined as those with daily rainfall  $\geq 26$  mm. This threshold was used to check the MJO impacts on extreme rainfall events statistics in Saudi Arabia during the wet season. The spatial density of meteorological observatories is low and uneven in some areas of Saudi Arabia. So, the ERA5 reanalysis high resolution ( $0.25^\circ \times 0.25^\circ$ ) gridded dataset, provided by the Copernicus Climate Change Service (C3S) of ECMWF, was also used to investigate the MJO local influence on daily total precipitation. The atmospheric variables like; daily total precipitation, mean sea level pressure (MSLP), OLR, geopotential height, U (zonal) and V (meridional) winds, specific humidity, mean temperature and latent heat of vaporization were obtained from ERA5 for the period 1985–2021. The ERA5 datasets offers a higher horizontal and vertical grid resolution in both space and time and assimilates more observational datasets than previous reanalysis, which makes it significantly more accurate (Hersbach et al. 2020). The daily parameters were constructed by averaging 6 hourly ERA5 dataset at synoptic hours (00, 06, 12 and 18 UTC). However, daily outgoing longwave radiation (OLR) was obtained from the National Oceanic and Atmospheric Administration (NOAA; Liebmann and Smith 1996).

## ii. Methodology

To understand the intraseasonal rainfall variability signal, the fast Fourier transformation (FFT) is applied to the time series of rainfall averaged over Saudi Arabia as a spectrum analysis to identify the dominant period. Before spectrum analysis, the annual cycle is removed from the Saudi Arabian daily average rainfall dataset by subtracting the climatological mean and linear trend during 1985–2021. The daily total precipitation gridded dataset obtained from ERA5 is used to analyze the wet season climatological distribution, variance, and influence of MJO phases on total precipitation distributions during wet season for the period 1985–2021. The MJO variability is characterized by the real-time multivariate (RMM) index (Wheeler and Hendon 2004; hereafter WH04), obtained from the Australian Bureau of Meteorology (<http://www.bom.gov.au/climate/mjo>). The MJO phase for each day is determined by the RMM index, a pair of PC time series called RMM1 and RMM2. The RMM index is calculated by using the following equation:

$$RMM = \sqrt{(RMM1^2 + RMM2^2)}.$$

There are eight MJO phases determined by using RMM index and this index is formed by the time series (RMM1, RMM2) associated with two empirical orthogonal functions

(EOFs). The combined EOFs are calculated by using long wave radiation (OLR), zonal winds at 850 and 200 hPa in the equatorial region (WH04). The intraseasonal anomalies were acquired by removing the climatological mean seasonal cycle by applying 30- to 90-day bandpass filter (Tian et al. 2017) on the ERA5 and OLR dataset. The composites of MJO cycle (eight phases) were calculated by averaging the daily anomalies that occurred within each phase. The MJO phase for each day is determined by using the MJO (RMM) index. The intraseasonal anomalies were composited into the two groups based on whether wetter or dryer conditions prevailed over Saudi Arabia. The MJO composites in this study were constructed using the RMM index with the condition that the amplitude must be greater than or equal to one standard deviation and the MJO phases must be in numerical order.

Based on WH04, the MJO intraseasonal anomaly composites were computed from different daily parameters such as mean temperatures, geopotential height, U (zonal) and V (meridional) winds, specific humidity, vertical velocity, latent heat of vaporization and mean sea level pressure (MSLP). These parameters were used to describe the physical mechanism associated with intraseasonal precipitation variability over Saudi Arabia. The area average ( $18\text{--}31^\circ \text{N}$ ;  $39\text{--}50^\circ \text{E}$ ) vertical integrated moisture flux (1000–200 hPa) and column-integrated moist static energy between the 1000–100 hPa levels were also calculated to describe the intraseasonal variations in atmospheric dynamics and thermodynamics. The statistical significance is calculated by using Student's *t* test of all spatial maps to describe the intraseasonal changes associated with MJO phases over Saudi Arabia.

## 3 Results and Discussion

### 3.1 Rainfall Variability During the Wet Season

The wet season (November to April) is not only the dominant season for the Middle East winter monsoon (Abid et al. 2016) but is also the active season for MJO, with a larger amplitude and more eastward-propagating events (Zhang 2005; Nazemosadat and Ghaedamini 2010; pourasghar et al. 2015) than the events observed in other seasons. The spatial distributions of rainfall climatological mean and standard deviation over the Arabian Peninsula for the wet season show that maximum rainfall occurs over central and southwestern parts of Saudi Arabia (Figs. 1a, b), where magnitudes are greater than 0.5 mm/day. This indicates that wet season rainfall variability in central and southwestern Saudi Arabia is much more substantial than in the other regions. Before the investigation of MJO influences on regional rainfall variabilities, it is important to understand

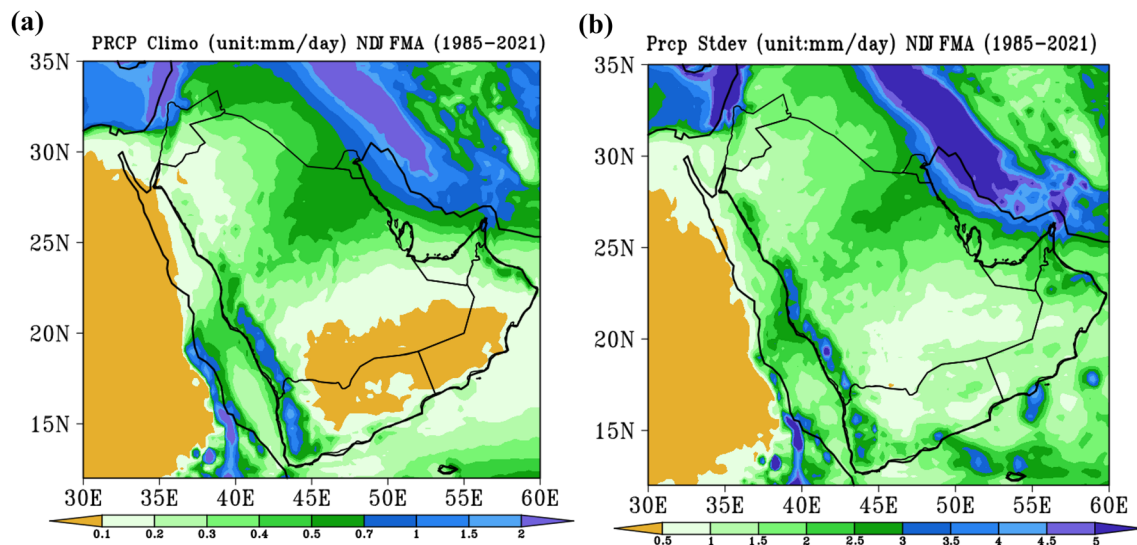


**Fig. 1** The ERA5 total precipitation (mm/day) shows **a** wet season (Nov–Apr) climatology and **b** standard deviation (Stdev) over the Arabian Peninsula during the period 1985–2021

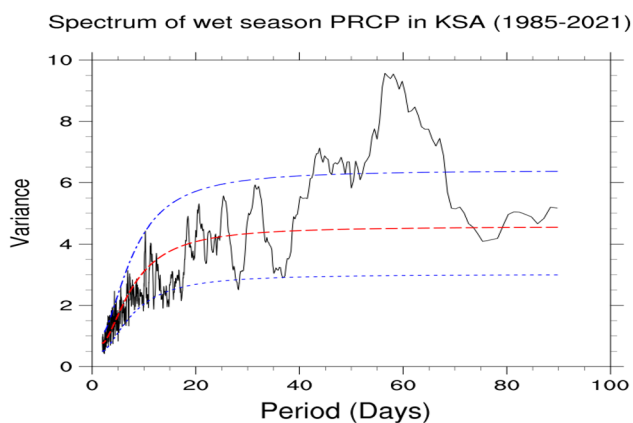


**Fig. 2** Power spectrum of wet season (Nov–April) rainfall over Saudi Arabia. Blue lines show the bandwidth, while the red line shows the noise spectrum. The annual cycle is removed before performing the spectrum analysis

the intraseasonal rainfall features. The characteristics of intraseasonal rainfall variations can be explained by using the power spectra analysis of daily rainfall anomalies (Cao and Wu 2017).

The power spectra of intraseasonal (1- to 91-day period) rainfall anomalies (Fig. 2) is performed for Saudi Arabia during the wet season. The observations power spectrum exhibits a peak (between 35 and 75 days) associated with intraseasonal oscillations, which is larger than the spectral level of red noise. This suggests that the intraseasonal rainfall variability in Saudi Arabia during the wet season is closely associated with the MJO activity other than the synoptic-scale disturbances. During the wet season, the region

experiences sometime extreme rainfall events, which may be attributed to the synoptic-scale disturbances (Kang et al. 2015) and MJO-associated disturbances (Pourasghar et al. 2015; Tippett et al. 2015). Therefore, the observed MJO index (WH04) is used to describe the wet and dry periods and their associated MJO phases over Saudi Arabia during the wet season. Analysis of the daily observational rainfall dataset shows that the probability of rainfall events during the wet season is only 4.68%, and the likelihood of extreme rainfall events during the same season is only 0.24%, representing the region's rainfall deficiency.

The statistical analysis of the observed rainfall dataset shows that rainfall events occur most frequently (41% of the total) during MJO phases 1, 2, 7, and 8 as compared to the MJO dry phases 3, 4, 5, and 6, which represent 23% of the total. Further, the frequency distribution of extreme rainfall events over Saudi Arabia shows that the probability of such events is high (46%) during the MJO phases 1, 2, 7, and 8 as compared to MJO phases 3, 4, 5 and 6, which have the corresponding possibility of only 18%. The percentage contribution to total rainfall and quantity of extreme rainfall events is also high during the MJO phases 1, 2, 7, and 8 (Fig. 3a). Altogether, 44% of total rainfall quantity occurred during the MJO phases 1, 2, 7, and 8 and 20% occurred during the MJO phases 3, 4, 5 and 6. Similarly, 46% of total quantity of extreme rainfall occurred during the MJO phases 1, 2, 7, and 8 and 16% during the MJO phases 3, 4, 5, and 6 (Fig. 3b). This analysis defined a rainfall event as one with daily rainfall  $\geq 1$  mm and extreme rainfall event as one with daily rainfall  $\geq 26$  mm reported at a station. The percentage contribution of rainfall (extreme rainfall) events to the total amount varies from phase to phase during MJO 8 phases in

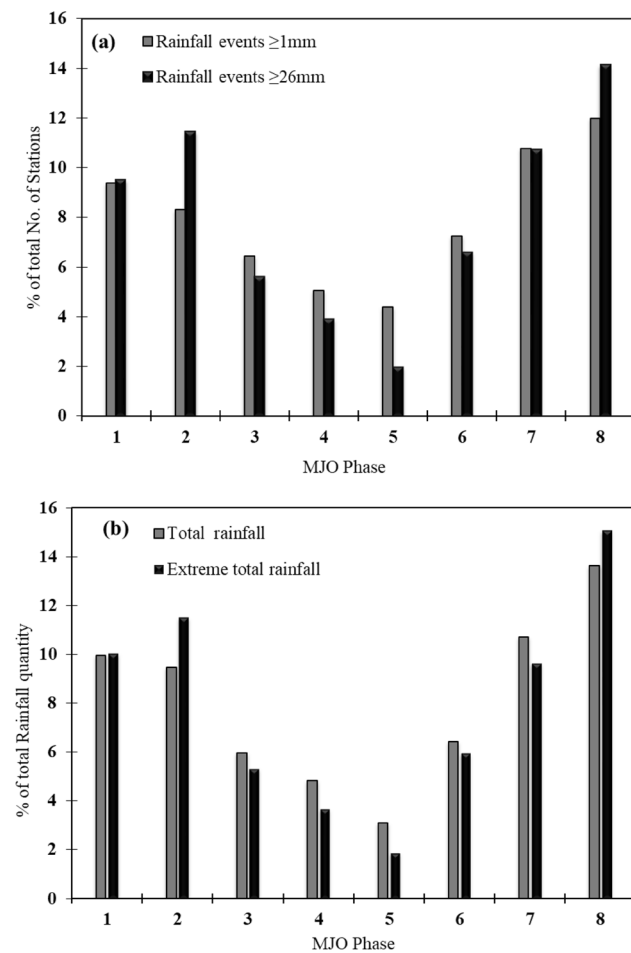


**Fig. 3** **a** The histogram of percentage (%) of total number of stations with normal and extreme rainfall events over Saudi Arabia during MJO 8 phases for the period 1985–2021. **b** Same as (a), except for total rainfall quantities received during normal and extreme rainfall events

the wet season. It is observed that the MJO phases 1, 2, 7, and 8 have a higher impact on the Saudi Arabian intraseasonal rainfall variability during wet season, as compared to the MJO phases 3, 4, 5, and 6. The MJO 8 phases also have a wave-like influence on rainfall events during the wet season (Fig. 3a, b). The statistical analysis shows that the region may receive a number of extreme rainfall events which may be attributed to the different MJO phases, as the dominant mode of intraseasonal variability.

Other than the observational rainfall dataset, the ERA5 reanalysis daily rainfall dataset is also investigated for intraseasonal rainfall variability in Saudi Arabia (Fig. 4) in support of observational analysis. The MJO phases categorized into wet and dry phases for Saudi Arabian intraseasonal rainfall variability based on positive and negative intraseasonal rainfall anomalies. The influence of MJO 8 phases is also investigated in the spatial distributions of daily total rainfall over Saudi Arabia (Figs. 4a–h). Positive rainfall anomalies

(Figs. 4a, b, g, h) are observed during the MJO phases 1, 2, 7, and 8 (hereafter named as wet phases), while negative rainfall anomalies (Figs. 4d–f) are found during the MJO phases 3, 4, 5, and 6 (hereafter named as dry phases). From the gridded precipitation data analysis, it is evident that the MJO 8 phases have significant influence on intraseasonal rainfall variability (Fig. 4a–h) during the wet season in central and southwestern parts of Saudi Arabia. The intraseasonal rainfall changes associated with the MJO phases are statistically significant at the 99% level and the statistical significance is calculated by using Student's *t* test.

In connection with the intraseasonal rainfall changes during MJO 8 phases, the mean sea level pressure (MSLP) and (U, V) 1000 hPa wind anomalies also change in the region (Fig. 5a–h). The typical sea-level pressure patterns over the Indian Ocean affect the moisture convergence and divergence. The region's negative and positive MSLP anomalies propagate from west to east during the MJO 8 phases with time evolution. Moisture transportation in the lower troposphere from the large ocean body is also connected with MSLP changes associated with wind speed and directions. The east–west changes in MSLP over Arabian Peninsula and Indian Ocean are observed in the region during MJO phases. In the MJO wet phases, high-pressure anomalies prevail over the Indian Ocean (Fig. 5a, b, g, h) and low-pressure anomalies over the Arabian Peninsula, which are favorable for moisture advection from the Arabian Sea into the Arabian Peninsula. The southerly and southeasterly winds push warm tropical moist air from North Arabian Sea into the Arabian Peninsula. This low-pressure dipole anomaly may favor an increased likelihood of intraseasonal rainfall events in the Arabian Peninsula during the wet season. In contrast, during MJO dry phases, a well-defined ridge of high-pressure anomalies prevails over the Arabian Peninsula, which causes moisture divergence from the region. This pattern do not favor the moisture advection into the Arabian Peninsula during the MJO dry phases (Fig. 5c–f). The intraseasonal MSLP changes associated with MJO 8 phases are statistically significant. Generally, high pressure over the Arabian Sea provides favorable conditions for moisture advection into the Arabian Peninsula, which may favor convection and cloud development due to the interaction of cold and warm air masses in Saudi Arabia. But decreased MSLP over the Indian Ocean or North Arabian Sea is not favorable to push the moisture fluxes into the Arabian Peninsula and may lead to dry conditions. The pressure gradient between the North Arabian Sea and Arabian Peninsula controls the precipitation distributions and rainfall events in the region, corresponding with changes during the MJO wet and dry phases. Winds coming from the south and southeast pick up moisture from the Arabian Sea and the Red Sea, enhancing the probability of extreme rainfall events in Saudi Arabia (De Vries et al. 2018). The possible physical

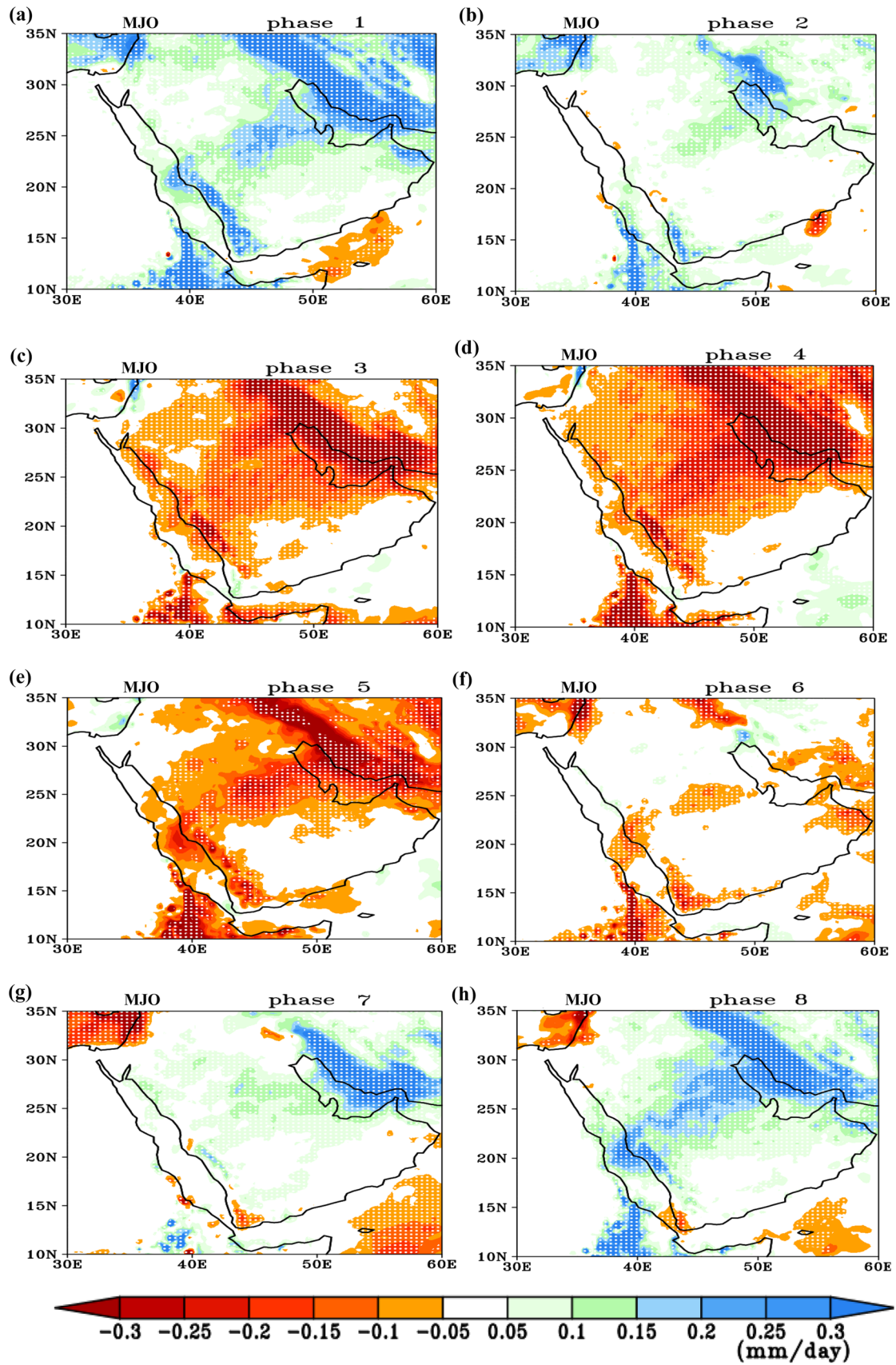


**Fig. 4 (a–h)** The intraseasonal rainfall (mm/day) anomaly composites during MJO 8 phases for the period 1985–2015. The changes are statistically significant (dotted areas) at the 99% level

mechanism associated with intraseasonal rainfall variability in Saudi Arabia during MJO wet and dry phases can be helpful to understand the MJO impacts on intraseasonal rainfall variability.

### 3.2 Physical Mechanism of the Intraseasonal Rainfall Variability

A comprehensive understanding of intraseasonal dynamic and thermodynamic variability of atmosphere over Saudi Arabia during the wet season requires analysis of how the MJO influences the intraseasonal rainfall changes. It is already shown (Seo et al. 2016; Abid et al. 2020) that tropical heating located over the Indian Ocean leads to surface cooling caused by local Hadley circulation over eastern Europe through meridional temperature advection due to poleward propagating Rossby waves. The upper-level intraseasonal circulation variability is explained by MJO induced teleconnections (Matthews et al. 2004; Seo and Son 2012; Cannon et al. 2017). The intraseasonal variabilities in upper-level circulations are examined for the purpose to analyze the connection between MJO wet and dry phases and regional atmospheric anomalies. The MJO composites of intraseasonal (30- to 90-day) filtered anomalies of stream function at 300 hPa (PSI300) and OLR during 1985–2021 are shown in (Fig. 6a, b). The stream function is a meteorological dynamical variable used to show the large-scale circulation response to the MJO 8 phases. The stream function are constructed by using U and V winds at 300 hPa level from ERA5. It is observed that the anomalous OLR patterns are linked with intraseasonal changes in the cloud development and atmospheric circulation patterns. There are significant negative OLR changes and negative stream function (dashed contours) associated with low geopotential height (cyclonic circulations) during the MJO wet phases (Fig. 6a). This pattern favors enhanced convection and precipitation in the region. However, during the MJO dry phases (Fig. 6b), the significant positive values of OLR and positive PSI300 (solid contours) associated with high geopotential height (anticyclonic circulation), which reflect suppressed convection and decreased precipitation anomalies in the region. These intraseasonal variations are consistent with recent observational studies (Cassou 2008; Guo et al. 2017). For example, Guo et al. 2017 found negative stream function at 250 hPa and positive storm frequency anomalies over the Middle East during MJO wet phases and vice versa for MJO dry phases. The atmospheric dynamical changes associated with MJO 8 phases play important role in intraseasonal rainfall variability in Saudi Arabia during the wet season. The

atmospheric circulations and OLR anomalies associated with MJO wet and dry phases may also correspond to intraseasonal changes in surface climatic variables in the region. The upper-level low- and high-pressure systems affect the horizontal moisture fluxes along their trajectories.

In recent studies it is mentioned that among other factors, the frequency and intensity of rainfall is directly linked to changes in vertical integrated moisture flux convergence (Hsu et al. 2016; Darand et al. 2019; Atif et al. 2020; Zhao et al. 2020). The moisture budget depends mainly on the changes in horizontal moisture flux convergence (MFC), which is proportional to the vertically integrated product of specific humidity and horizontal mass convergence through the troposphere.

The vertically integrated moisture flux convergence (VIMFC) is represented by Eq. (1).

$$VIMFC = -\frac{1}{g} \int_{p_0}^{p_t} \left( \frac{\partial uq}{\partial x} + \frac{\partial vq}{\partial y} \right) dp, \quad (1)$$

where  $q$  is the specific humidity,  $u$  (zonal) and  $v$  (meridional) are the wind components along  $x$  and  $y$  directions,  $p$  is the pressure,  $p_0$  is the surface pressure,  $p_t$  is the pressure at the top of the atmosphere layer, and  $g$  is the acceleration due to the gravity. The VIMFC is calculated by summation of the horizontal moisture flux convergence between the levels 1000–200 hPa. The intraseasonal changes (Fig. 7a, b) in VIMFC with respect to the climatology are calculated by using Eq. 1 and the values are expressed in units of  $10^{-5}$  kg/s.m<sup>2</sup>. The 850 hPa (QU, QV) vectors are used to show the lower-level moisture advection. The positive values show the convergence and negative values to divergence in intraseasonal VIMFC during the MJO wet and dry phases. The intraseasonal changes described above that occurred during the MJO wet and dry phases are also reflected in the VIMFC changes. It is observed that the significant positive anomalies of vertical integrated moisture convergence over the central parts of Saudi Arabia play an important role in providing favorable conditions for cloud development and rainfall events during the MJO wet phases (Fig. 7a). During these phases, the cyclonic circulation over the central and northern parts of Saudi Arabia can enhance moisture convergence from the tropical Africa and Indian Ocean. The subtropical jet stream penetrates toward the lower latitudes from its mean position (Supplementary Fig. 1a) during the MJO wet phases. The southward shift of subtropical jet intensifies the cyclonic circulation and enhances moisture convergence in the region (Tubi et al. 2017). The primary source of moisture flux is through the Arabian Sea, with an anomalous anticyclonic flow over the Arabian Sea. During MJO dry phases (Fig. 7b), significant negative anomalies of vertical integrated moisture divergence over most parts of Saudi Arabia prevail accompanied by anomalous anticyclonic circulation,

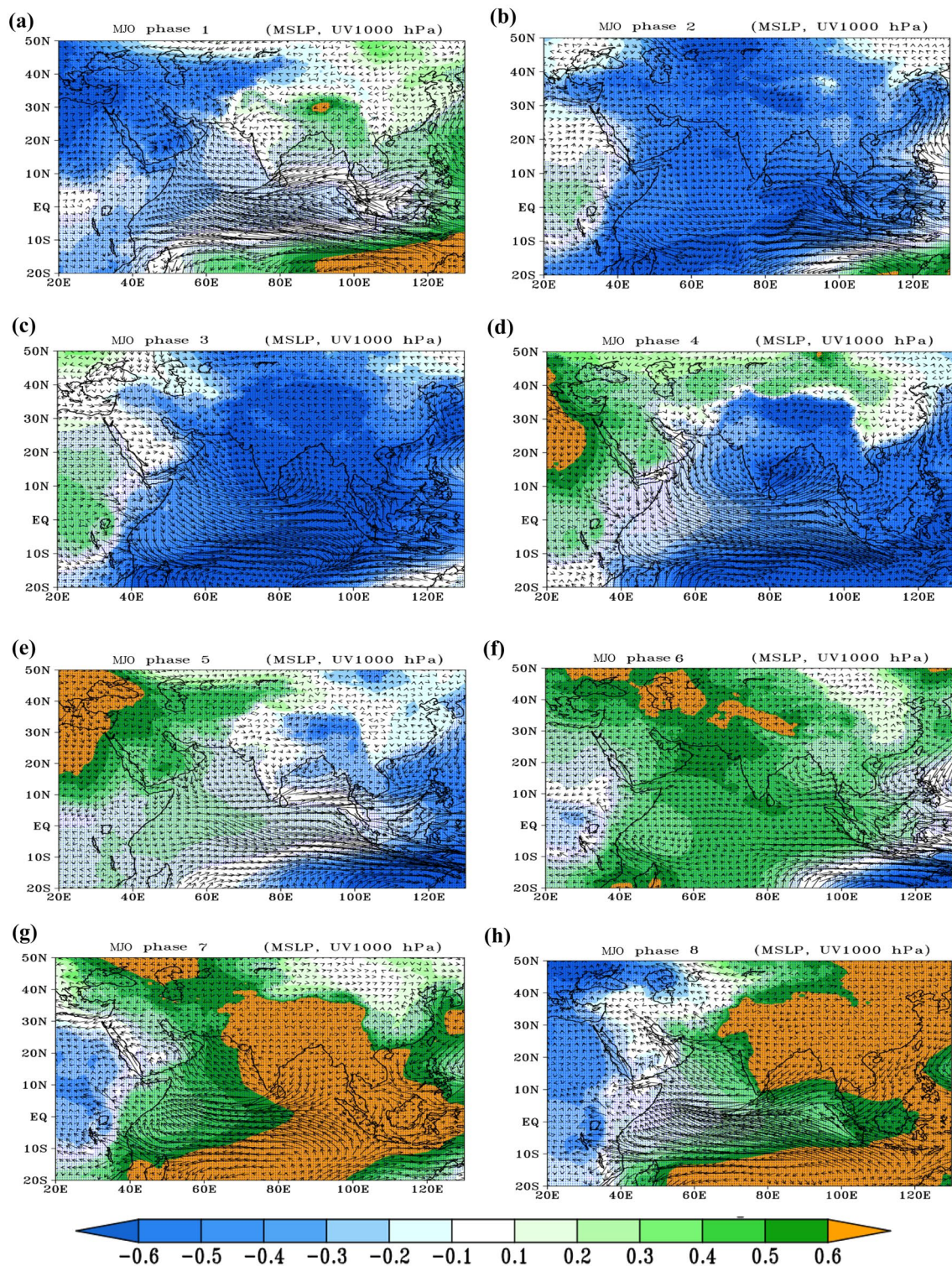


**Fig. 5** (a–h) The intraseasonal anomaly composites of MSLP (shaded, unit: mb) and 1000 hPa winds (vectors) during the MJO 8 phases. The changes are significant (dotted areas) at the 99% level

which suppress the moisture advection into the region. The subtropical jet stream shifts toward the higher latitudes from its mean position (Supplementary Fig. 1b) during the MJO

dry phases. The northward shift of subtropical jet enhances the anticyclonic circulation and enhances moisture divergence in the region. This may lead to the drier conditions



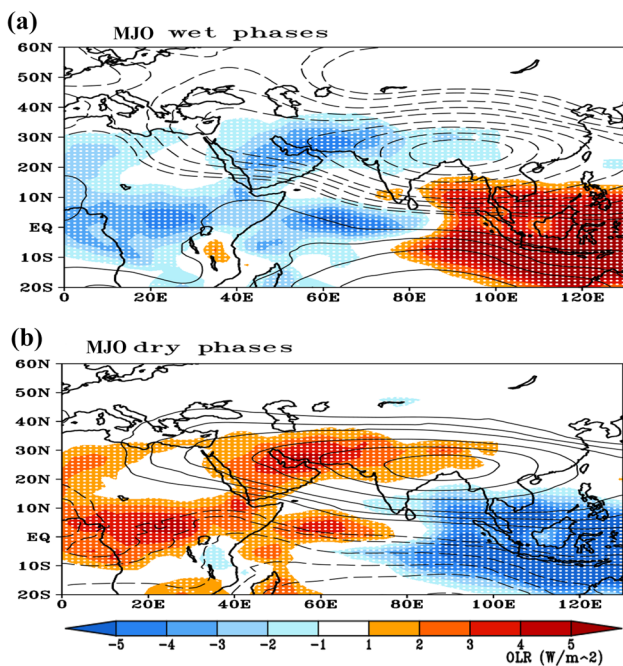


**Fig. 6** The intraseasonal composites of stream function (PSI300, contour intervals are  $1 \times 10^6 \text{ m}^2 \text{ s}^{-1}$ , starting at  $\pm 5 \times 10^6 \text{ m}^2 \text{ s}^{-1}$ ) and OLR (shaded colors;  $\text{Wm}^{-2}$ ) for **a** MJO wet phases and **b** MJO dry phases. The red colors correspond to decreased convection activity and are associated with drier conditions, while blue shaded colors link to enhanced convection activity and wetter conditions. Solid contours represent anticyclonic circulations (high geopotentials), while dashed contours represent cyclonic circulations (low geopotentials). The changes are significant (dotted areas) at the 99% level

and less probability of extreme rainfall events during the MJO dry phases. All the previous analyses are consistent and show that intraseasonal changes in upper air circulations and moisture fluxes in the region are influenced by the MJO events. The changes in rainfall, atmospheric circulation and moisture flux anomalies at intraseasonal timescales occur with time evaluation of MJO 8 phases. The pairing of MJO events supports that Saudi Arabia may receive above than normal rainfall during the MJO wet phases, and below than normal during the dry phase.

To further support the combination of MJO 8 phases with reference to the intraseasonal rainfall variability in Saudi Arabia, the analysis of area average ( $18\text{--}31^\circ \text{ N}$ ;  $39\text{--}50^\circ \text{ E}$ ) vertical motion of atmosphere is investigated. The vertical pressure velocity ( $-\omega$ ; as seen in Fig. 8a) and vertical profile of moisture advection ( $-\omega * \frac{dq}{dp}$ ; as seen in Fig. 8b) with respect to their climatologies are associated with the positive and negative changes in intraseasonal rainfall (Loriaux et al. 2016) over Saudi Arabia. The omega vertical profile is an indirect measure of the large-scale convergence over the region. From Saudi Arabian station-based observational rainfall analysis (Fig. 3) and

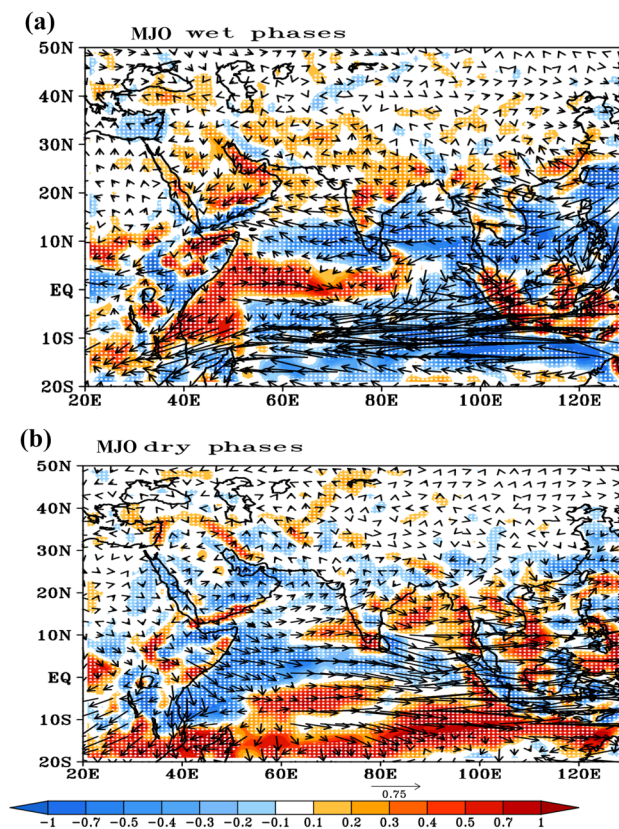


**Fig. 7** The vertically integrated moisture flux divergence (blue), convergence (red) and in the shaded regions (unit:  $10^{-5} \text{ kg/s.m}^2$ ) the vector shows the moisture advection at 850 hPa (unit: 0.75, s.g/kg) during MJO **a** wet phases and **b** dry phases. The changes are statistically significant (dotted areas) at the 99% level

gridded reanalysis rainfall (Fig. 4), the vertical motion is expected to rise during the MJO wet phases and sink during the dry phases. It is observed that during the MJO wet phases, the vertical velocity of atmosphere increases more as compared to the vertical velocity of the atmosphere during the MJO dry phases (Fig. 8a). The vertical advection of moisture increases (decreases) with respect to the vertical profile of omega changes during the MJO wet (dry) phases, as shown in Fig. 8b. The precipitation associated with shallow and deep convection largely depends on how high convection can develop along the vertical direction. The rising motion and positive vertical moisture advection above than normal are clearly observed during the MJO wet phases, which may lead to positive intraseasonal rainfall anomalies in Saudi Arabia. However, sinking motion and negative vertical moisture advection above than normal at all levels (1000 – 100 hPa) lead to the negative intraseasonal rainfall anomalies in the region during the MJO dry phases in the wet season. The intraseasonal rising (sinking) motion and enhanced (suppressed) vertical moisture advection over Saudi Arabia during the

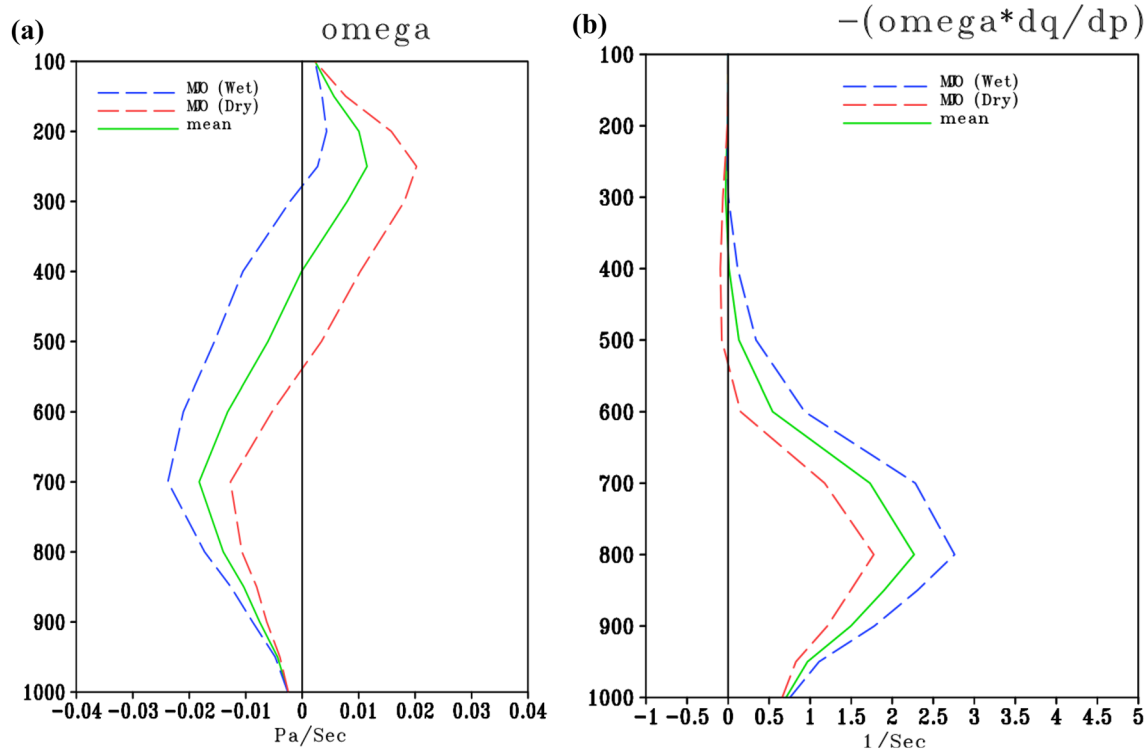


**Fig. 8** **a** The area average (18–31° N; 39–50° E) vertical pressure velocity profiles. **b** The vertical profile of area average (18–31° N; 39–50° E) moisture advection (units:  $10^{-9}/s$ ). MJO wet phases in blue and dry phases in red are shown

MJO wet (dry) phases can be associated with intraseasonal changes in atmospheric circulation and VIMFC anomalies described in the above analysis. Other than the vertical profiles of moisture advection, the column-integrated moist static energy (MSE) budget is largely used to study the MJO impacts on rainfall (Arnold et al. 2013; Sobel et al. 2014). The horizontal MSE and vertical MSE advection contributes to the heavy rainfall events associated with large-scale atmospheric circulations (Zheng et al. 2020). To assess the intraseasonal vertical characteristics within the tropospheric column 1000 – 100 hPa levels, the area average (18–31° N; 39–50° E) moist static energy (MSE) over Saudi Arabia during MJO 8 phases is calculated by using the equation:

$$\text{Moist static energy} = CpT + gz + Lq. \quad (2)$$

The MSE (Eq. 2) is calculated using the filtered specific heat of dry air at constant pressure  $Cp$ , temperature  $T$ , gravity acceleration  $g$ , geopotential height  $z$ , specific humidity  $q$ , and latent heat of vaporization  $L$ . MSE is preserved for unmixed parcel ascent. During the MJO wet phases, the moist static energy increases above normal and causes more instability. However, during MJO dry phases, the MSE decreases to below average and causes

less instability. A high bias of MSE near the surface and a low bias of MSE in the upper atmosphere allow climatically favorable conditions for tropospheric convection over Saudi Arabia, which leads to above normal precipitation during the MJO wet phases and vice versa during the MJO dry phases (Fig. 9). The analysis of vertical characteristics of the atmosphere over the region are consistent with the previous analysis.

Finally, the combined impact of the MJO wet and dry phases is reflected in the precipitation over Saudi Arabia. As mentioned earlier (see too Fig. 1b), rainfall shows the highest variance in central and southwestern parts of Saudi Arabia. So, the MJO associated wet and dry phases also strongly influence intraseasonal rainfall variability during the wet season in the central and southwestern parts of the Peninsula. During the MJO wet phases, conditions are significantly wetter (Fig. 10a); however, conditions are significantly dryer (Fig. 10b) during the MJO dry phases. These precipitation anomalies support all the analyses of this study and confirm that the MJO wet and dry phases significantly influence intraseasonal rainfall variability in Saudi Arabia's wet season.

All the above-mentioned observational findings reflect the significant influence of MJO on intraseasonal rainfall variability in Saudi Arabia. In addition, the analysis

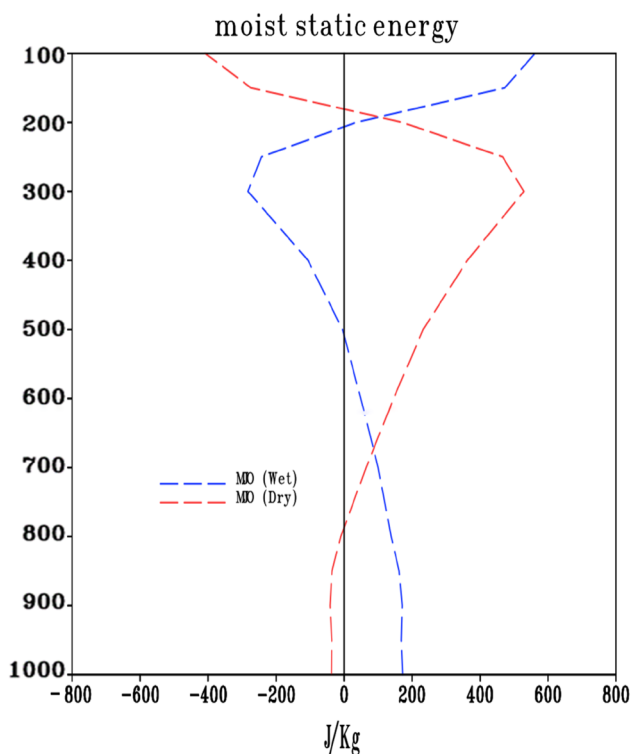


**Fig. 9** The intraseasonal anomaly composites of vertical profile of area average (18–31° N; 39–50° E) moist static energy over Saudi Arabia during the wet season. MJO wet phases in blue and dry phases in red are shown

is consistent with recent studies (e.g., Tippett et al. 2015; Pourasghar et al. 2015; Nazemosadat et al. 2017; Sreekala et al. 2018) describing MJO influence on intraseasonal climate variability of the region.

### 4 Summary and Conclusions

The impact of MJO on Saudi Arabian intraseasonal rainfall variability is investigated during the wet season (November–April) for the period 1985–2021. The maximum interannual rainfall variability is observed over the central and southwestern parts of Saudi Arabia. Extensive intraseasonal rainfall variability changes were observed during the MJO 8 phases over Saudi Arabia. These changes are linked to the MJO convection centers propagating eastward from the tropical Indian Ocean to the Central Pacific, as discerned by using the RMM index from the Australian Bureau of Meteorology. This is due to changes observed in intraseasonal rainfall during the MJO 8 phases in the tropical regions around the globe. Among the two paired phases of MJO, phases 1, 2, 7, and 8, and 3, 4, 5, and 6 can be identified as the typical wet and dry phases, respectively. The large-scale atmospheric circulation anomalies and moisture flux transport processes are analyzed to explore the physical mechanism of the impacts associated with MJO signals. For the MJO wet phases, negative stream function and OLR anomalies develop over the region. During the wet phases,

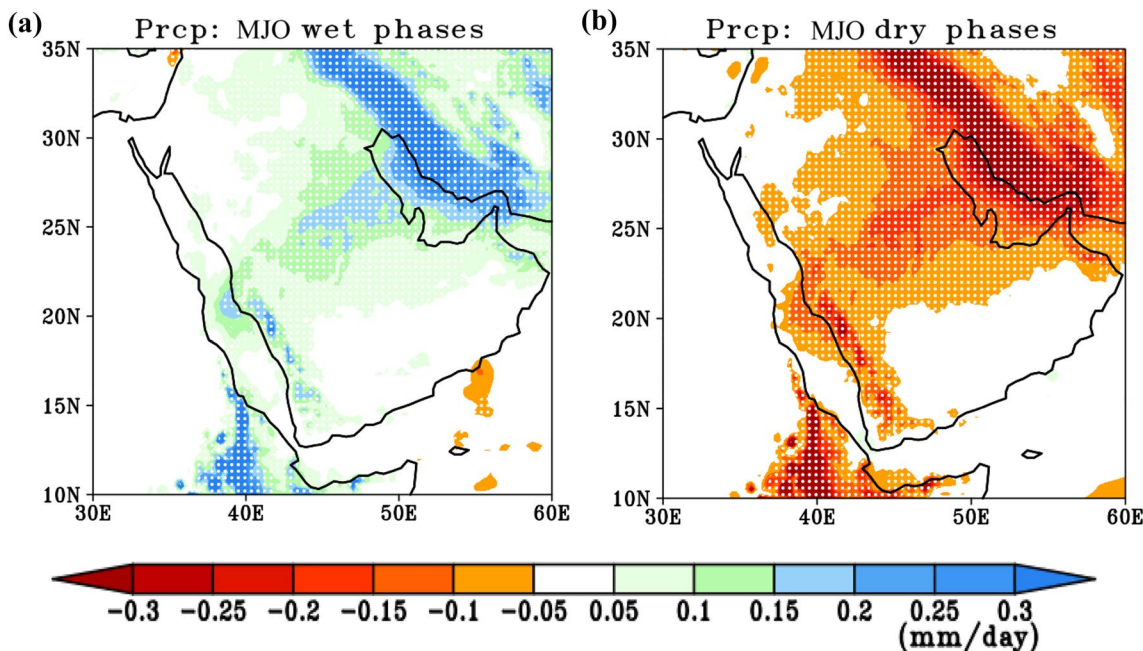


**Fig. 10** The intraseasonal anomaly composites of precipitation (mm/day) during MJO **a** wet phases and **b** dry phases for the period 1985–2021. The changes are statistically significant (dotted areas) at the 99% level

these cyclonic circulation anomalies over South Asia in the upper troposphere contribute significantly to the anomalous moisture transport from the Arabian Sea into the Arabian Peninsula. The high MSLP anomalies over the Arabian Sea and low MSLP anomalies over the Arabian Peninsula favor the moisture flux transport from the Arabian Sea. In contrast, for the MJO dry phases, positive stream function and OLR anomalies develop over the region, representing a reduction of convection.

The anticyclonic circulation anomalies (high pressure) over South Asia in the upper troposphere during the dry phases may reduce the anomalous moisture transport from the Arabian Sea into the Arabian Peninsula. The high MSLP anomalies over the Arabian Peninsula and low MSLP anomalies over the Arabian Sea favor reducing moisture flux transport from the Arabian Sea. The MJO events in the wet season impact the occurrence of extreme rainfall events in Saudi Arabia, mainly by modulating the atmospheric circulation anomalies and the moisture fluxes accompanying the wind anomalies coming from the Arabian and Red Seas. The upward motion and vertical moisture advection enhanced by the convergence of moisture provide favorable conditions for wetter conditions over Saudi Arabia. The physical analysis reveals that intraseasonal changes in horizontal moisture convergence, vertical moisture advection, and moist static energy may serve as potential indicators for wetter conditions in the region. The relationship between MJO and intraseasonal rainfall changes during the wet season is discussed in this study and has important implications for the intraseasonal rainfall predictability in Saudi Arabia.

This study explains the influence of the MJO phases on the occurrence of intraseasonal rainfall variability in Saudi Arabia during the wet season. In recent studies (e.g., Jeong et al. 2005; Rodney et al. 2013; Zhao et al. 2013; Pourasghar et al. 2015), it has been found that MJO phases significantly influence the magnitude of surface air temperature anomalies. So, it is worthwhile to investigate in the future whether or not the MJO phases have a comparable impact on intraseasonal surface air temperatures variabilities in Saudi Arabia.

**Supplementary Information** The online version contains supplementary material available at <https://doi.org/10.1007/s41748-022-00334-w>.

**Acknowledgements** The author would like to extend his regards and acknowledge to the Center of Excellence for Climate Change Research (CECCR), King Abdulaziz University, for supporting this research work. The NCM is acknowledged for providing observational daily rainfall station dataset. Computation work described in this paper was performed using Aziz Supercomputer at King Abdulaziz University's High Performance Computing Center, Jeddah, Saudi Arabia.

**Funding** There is no funding for this research.

**Data availability** The observational data used in this study belongs to NCM and not available to share.

## Declarations

**Conflict of Interest** The authors declare that they have no conflict of interest.

**Open Access** This article is licensed under a Creative Commons Attribution 4.0 International License, which permits use, sharing, adaptation, distribution and reproduction in any medium or format, as long as you give appropriate credit to the original author(s) and the source, provide a link to the Creative Commons licence, and indicate if changes were made. The images or other third party material in this article are included in the article's Creative Commons licence, unless indicated otherwise in a credit line to the material. If material is not included in the article's Creative Commons licence and your intended use is not permitted by statutory regulation or exceeds the permitted use, you will need to obtain permission directly from the copyright holder. To view a copy of this licence, visit <http://creativecommons.org/licenses/by/4.0/>.

## References

- Abid MA (2018) ENSO relationship to summer rainfall variability and its potential predictability over Arabian Peninsula region. *Npj Clim Atmos Sci*. <https://doi.org/10.1038/s41612-017-0003-7>
- Abid MA, Kucharski F, Almazroui M, Kang IS (2016) Interannual rainfall variability and ECMWF-Sys4-based predictability over the Arabian Peninsula winter monsoon region. *QJR Met Soc* 142(694):233–242. <https://doi.org/10.1002/qj.2648>
- Abid MA, Ashfaq M, Kucharski F, Evans KJ, Almazroui M (2020) Tropical Indian Ocean mediates ENSO influence over central Southwest Asia rainfall during the wet season. *Geophys Res Lett*. <https://doi.org/10.1029/2020GL089308>
- Alaka G, Maloney E (2012) The influence of the MJO on upstream precursors to African easterly waves. *J Clim* 25:3219–3236. <https://doi.org/10.1175/JCLI-D-11-00232.1>
- Almazroui M (2011) Calibration of TRMM rainfall climatology over Saudi Arabia during 1998–2009. *Atmos Res* 99(2011):400–414. <https://doi.org/10.1016/j.atmosres.2010.11.006>
- Almazroui M (2020) Rainfall trends and extremes in Saudi Arabia in recent decades. *Atmos* 11(9):964. <https://doi.org/10.3390/atmos11090964>
- Almazroui M, Awad AM, Islam MN et al (2015) A climatological study: wet season cyclone tracks in the East Mediterranean region. *Theor Appl Climatol* 120:351–365. <https://doi.org/10.1007/s00704-014-1178-z>
- Almazroui M, Islam MN, Saeed S et al (2020) Future changes in climate over the Arabian Peninsula based on CMIP6 multimodel simulations. *Earth Syst Environ* 4:611–630. <https://doi.org/10.1007/s41748-020-00183-5>
- Arnold NP, Kuang Z, Tziperman E (2013) Enhanced MJO-like variability at high SST. *J Clim* 26(3):988–1001. <https://doi.org/10.1175/JCLI-D-12-00272.1>
- Atif RM, Almazroui M, Saeed S, Abid MA, Islam MN, Ismail M (2020) Extreme precipitation events over Saudi Arabia during the wet season and their associated teleconnections. *Atmos Res*. <https://doi.org/10.1016/j.atmosres.2019.104655>
- Barlow M, Wheeler M, Lyon B, Cullen H (2005) Modulation of daily precipitation over southern Asia by the Madden-Julian oscillation. *Mon Wea Rev* 133:3579–3594. <https://doi.org/10.1175/MWR3026.1>
- Cannon F, Carvalho L, Jones C, Hoell A, Norris J, Kiladis GN, Tahir AA (2017) The influence of tropical forcing on extreme winter precipitation in the western Himalaya. *Clim Dyn* 48(3):1213–1232. <https://doi.org/10.1007/s00382-016-3137-0>

- Cao X, Wu RG (2017) Origins of intraseasonal rainfall variations over the southern South China Sea in boreal winter. *Atmosph and Ocean Sci Lett* 10(1):44–50. <https://doi.org/10.1080/16742834.2017.1232584>
- Cassou C (2008) Intraseasonal interaction between the Madden–Julian oscillation and the North Atlantic oscillation. *Nat* 455(7212):523. <https://doi.org/10.1038/nature07286>
- Darand M, Pazhoh F (2019) Vertically integrated moisture flux convergence over Iran. *Clim Dyn* 53(5):3561–3582. <https://doi.org/10.1007/s00382-019-04726-z>
- De Vries AJ, Feldstein SB, Riemer M, Tyrlis E, Sprenger M, Baumgart M, Fnais M, Lelieveld J (2016) Dynamics of tropical-extratropical interactions and extreme precipitation events in Saudi Arabia in autumn, winter and spring. *Q J R Meteor Soc* 142:1862–1880. <https://doi.org/10.1002/qj.2781>
- De Vries AJ, Ouwersloot HG, Feldstein SB, Riemer M, El Kenawy AM, McCabe MF, Lelieveld J (2018) Identification of tropical-extratropical interactions and extreme precipitation events in the middle east based on potential vorticity and moisture transport. *JGR Atmosph* 123(2):861–881. <https://doi.org/10.1002/2017JDO27587>
- Ehsan MA, Tippett MK, Almazroui M et al (2017) Skill and predictability in multimodel ensemble forecasts for Northern Hemisphere regions with dominant winter precipitation. *Clim Dyn* 48:3309–3324. <https://doi.org/10.1007/s00382-016-3267-4>
- Flaounas E, Davolio S, Raveh-Rubin S, Pantillon F, Miglietta MM, Gaertner MA, Hatzaki M, Homar V, Khodayar S, Korres G, Kotroni V (2022) Mediterranean cyclones: current knowledge and open questions on dynamics, prediction, climatology and impacts. *Weath and Clim Dyn* 3(1):73–208. <https://doi.org/10.5194/wcd-3-173-2022>
- Guo Y, Shinoda T, Lin J, Chang EK (2017) Variations of Northern Hemisphere storm track and extratropical cyclone activity associated with the Madden–Julian oscillation. *J Clim* 30(13):4799–4818. <https://doi.org/10.1175/JCLI-D-16-0513.1>
- Haggag M, El-Badry H (2013) Mesoscale numerical study of quasi-stationary convective system over Jeddah in November 2009. *Atmos Clim Sci*. <https://doi.org/10.4236/acs.2013.31010>
- Han W, Webster PJ, Lin JL, Liu T, Fu R, Yuan D, Hu A (2008) Dynamics of interseasonal sea level and thermocline variability in the equatorial Atlantic during 2002–03. *J Phy Ocean* 38:945–967. <https://doi.org/10.1175/2008JPO3854.1>
- Hendon HH, Zhang C, Glick JD (1999) Interannual variation of the Madden–Julian oscillation during austral summer. *J Clim* 12(8):2538–2550. [https://doi.org/10.1175/1520-0442\(1999\)012%3c2538:IVOTMJ%3e2.0.CO;2](https://doi.org/10.1175/1520-0442(1999)012%3c2538:IVOTMJ%3e2.0.CO;2)
- Hersbach H, Bell B, Berrisford P, Hirahara S, Horányi A, Muñoz-Sabater J, Nicolas J, Peubey C, Radu R, Schepers D, Simmons A (2020) The ERA5 global reanalysis. *QRJ* 146(730):1999–2049. <https://doi.org/10.1002/qj.3803>
- Hsu PC, Lee JY, Ha KJ (2016) Influence of boreal summer intraseasonal oscillation on rainfall extremes in southern China. *Int J Climatol* 36:1403–1412. <https://doi.org/10.1002/joc.4433>
- Jafar Nazemosadat M, Shahgholian K (2017) Heavy precipitation in the southwest of Iran: association with the Madden–Julian oscillation and synoptic scale analysis. *Clim Dyn* 49(9):3091–3109. <https://doi.org/10.1007/s00382-016-3496-6>
- Jeong JH, Ho CH, Kim BM, Kwon WT (2005) Influence of the Madden–Julian oscillation on wintertime surface air temperature and cold surges in East Asia. *J Geophys Res Atmos*. <https://doi.org/10.1029/2004JD005408>
- Jia X, Chen LJ, Ren FM, Li CY (2011) Impact of the MJO on winter rainfall and circulation in China. *Adv Atmos Sci* 28:521–533. <https://doi.org/10.1007/s00376-010-9118-z>
- Kamil S, Almazroui M, Kucharski F, Kang IS (2017) Multidecadal changes in the relationship of storm frequency over Euro-Mediterranean Region and ENSO during boreal winter. *Earth Syst Environ* 1(1):6. <https://doi.org/10.1007/s41748-017-0011-0>
- Kang IS, Rashid IU, Kucharski F, Almazroui M, Alkhalaf AA (2015) Multi-decadal changes in the relationship between ENSO and wet-season precipitation in the Arabian Peninsula. *J Clim* 28:4743–4752. <https://doi.org/10.1175/JCLI-D-14-00388.1>
- Liebmann B, and Smith CA (1996) Description of a complete (interpolated) outgoing longwave radiation dataset. *Bul AMS* 77(6), 1275–1277. <https://www.jstor.org/stable/26233278>
- Loriaux J, Lenderink G, Siebesma AP (2016) Peak precipitation intensity in relation to atmospheric conditions and large-scale forcing at midlatitudes. *J Geophys Res Atmos* 121:5471–5487. <https://doi.org/10.1002/2015JD024274>
- Madden RA, Julian P (1971) Detection of a 40–50 day oscillation in the zonal wind. *J Atmosph Sci* 28:702–708. [https://doi.org/10.1175/1520-0469\(1971\)028%3c0702:DOADOI%3e2.0.CO;2](https://doi.org/10.1175/1520-0469(1971)028%3c0702:DOADOI%3e2.0.CO;2)
- Madden RA, Julian PR (1972) Description of global-scale circulation cells in the tropics with a 40–50 day period. *J Atmos Sci* 29:1109–1123. [https://doi.org/10.1175/1520-0469\(1972\)029%3c1109:DOGSCC%3e2.0.CO;2](https://doi.org/10.1175/1520-0469(1972)029%3c1109:DOGSCC%3e2.0.CO;2)
- Madden RA, Julian PR (1994) Observations of the 40–50-day tropical oscillation—a review. *Mon Weather Rev* 122(5):814–837. [https://doi.org/10.1175/1520-0493\(1994\)122%3c0814:OOTDIO%3e2.0.CO;2](https://doi.org/10.1175/1520-0493(1994)122%3c0814:OOTDIO%3e2.0.CO;2)
- Matthews AJ, Hoskins BJ, Masutani M (2004) The global response to tropical heating in the Madden–Julian oscillation during the northern winter. *Quart J RMS* 130:1991–2011. <https://doi.org/10.1256/qj.02.123>
- Merryfield WJ, Baehr J, Batté L, Becker EJ, Butler AH, Coelho CA, Danabasoglu G, Dirmeyer PA, Doblas-Reyes FJ, Domeisen DI, Ferranti L (2020) Current and emerging developments in subseasonal to decadal prediction. *Bul AMS* 101(6):E869–E896. <https://doi.org/10.1175/BAMS-D-19-0037.1>
- Nazemosadat MJ, Ghaedamini H (2010) On the relationships between the Madden–Julian oscillation and precipitation variability in southern Iran and the Arabian Peninsula: atmospheric circulation analysis. *J Clim* 23:887–904. <https://doi.org/10.1175/2009JCLI2141.1>
- Pai DS, Jyoti B, Sreejith OP, Hatwar HR (2011) Impact of MJO on the intraseasonal variation of summer monsoon rainfall over India. *Clim Dyn* 36:41–55. <https://doi.org/10.1007/s00382-009-0634-4>
- Pinto JG, Zacharias S, Fink AH, Leckebusch GC, Ulbrich U (2009) Factors contributing to the development of extreme North Atlantic cyclones and their relationship with the NAO. *Clim Dyn* 32(711–737):2009. <https://doi.org/10.1007/s00382-008-0396-4>
- Pohl B, Camberlin P (2006) Influence of Madden–Julian oscillation on East Africa rainfall I: intraseasonal variability and regional dependency. *QJR* 132:2521–2539. <https://doi.org/10.1256/qj.05.104>
- Pourasghar F, Tozuka T, Ghaemi H, Oettli P, Jahanbakhsh S, Yamagata T (2015) Influences of the MJO on intraseasonal rainfall variability over southern Iran. *Atmos Sci Lett* 16:110–118. <https://doi.org/10.1002/asl2.531>
- Raible CC (2007) On the relation between extremes of midlatitude cyclones and the atmospheric circulation using ERA40. *GRL* 34(L07703):2007. <https://doi.org/10.1029/2006GL029084>
- Ren HL, Ren P (2017) Impact of Madden–Julian oscillation upon winter extreme rainfall in Southern China: observations and predictability in CFSv2. *Atmosphere* 8:192. <https://doi.org/10.3390/atmos8100192>
- Rodney M, Lin H, Derome J (2013) Subseasonal prediction of wintertime North American surface air temperature during strong MJO

- events. *Mon Wea Rev* 141:2897–2909. <https://doi.org/10.1175/MWR-D-12-00221.1>
- Saeed S, Almazroui M (2019) Impacts of mid-latitude circulation on winter precipitation over the Arabian Peninsula. *Clim Dyn* 53(9):5253–5264. <https://doi.org/10.1007/s00382-019-04862-6>
- Saeed S, Kucharski F, Almazroui M (2022) Impacts of mid-latitude circulation on winter temperature variability in the Arabian Peninsula: the explicit role of NAO. *Clim Dyn* 1–18
- Schwartz C, Garfinkel CI (2017) Relative roles of the MJO and stratospheric variability in North Atlantic and European winter climate. *J Geophys Res Atmos* 122(8):4184–4201. <https://doi.org/10.1002/2016JD025829>
- Seo LHJ, Frierson DMW (2016) Unraveling the teleconnection mechanisms that induce wintertime temperature anomalies over the Northern Hemisphere continents in response to the MJO. *J Atmos Sci* 73:3557–3571. <https://doi.org/10.1175/JAS-D-16-0036.1>
- Seo KH, Son SW (2012) The global atmospheric circulation response to tropical diabatic heating associated with the Madden–Julian oscillation during northern winter. *J Atmos Sci* 69:79–96. <https://doi.org/10.1175/2011JAS3686.1>
- Slingo JM, Rowell DP, Sperber KR, Nortley F (1999) On the predictability of the interannual behaviour of the Madden-Julian oscillation and its relationship with El Niño. *QJR* 125(554):583–609. <https://doi.org/10.1002/qj.49712555411>
- Sobel A, Wang S, Kim D (2014) Moist static energy budget of the MJO during DYNAMO. *J Atmosph Sci* 71(11):4276–4291. <https://doi.org/10.1175/JAS-D-14-0052.1>
- Sreekala PP, Rao S, Rajeevan K, Arunachalam MS (2018) Combined effect of MJO, ENSO and IOD on the intraseasonal variability of northeast monsoon rainfall over south peninsular India. *Clim Dyn* 51(9):3865–3882. <https://doi.org/10.1007/s00382-018-4117-3>
- Tian B, Waliser DE, Kahn RA, Wong S (2011) Modulation of Atlantic aerosols by the Madden-Julian oscillation. *JGR: Atmos*. <https://doi.org/10.1029/2010JD015201>
- Tian D, Wood EF, Yuan X (2017) CFSv2-based sub-seasonal precipitation and temperature forecast skill over the contiguous United States. *Hydrol Earth Syst Sci* 21(3):1477–1490
- Tippett M, Almazroui M, Kang IS (2015) Extended-range forecasts of areal-averaged Saudi Arabia rainfall. *Weath Forecast* 30:1090–1105. <https://doi.org/10.1175/WAF-D-15-0011.1>
- Tubi A, Dayan U, Lensky IM (2017) Moisture transport by tropical plumes over the Middle East: a 30-year climatology. *QJR* 143(709):3165–3176. <https://doi.org/10.1002/qj.3170>
- Vigaud N, Tippett MK, Robertson AW (2019) Deterministic skill of subseasonal precipitation forecasts for the East Africa–West Asia sector from September to May. *JGR: Atmos* 124(22):11887–11896. <https://doi.org/10.1029/2019JD030747>
- Wheeler MC, Hendon HH (2004) An all-season real-time multivariate MJO index: development of an index for monitoring and prediction. Bureau of Meteorology Research Centre, Melbourne, Australia. *Mon Wea Rev* 132:1917–1932. [https://doi.org/10.1175/1520-0493\(2004\)132<1917:AMJOI>2.0.CO;2](https://doi.org/10.1175/1520-0493(2004)132<1917:AMJOI>2.0.CO;2)
- Wheeler MC, Hendon HH, Sam C, Holger M, Alexis D (2009) Impacts of the Madden-Julian oscillation on Australian rainfall and circulation. *J Clim* 22:1482–1498. <https://doi.org/10.1175/2008JCLI2595.1>
- Whitaker JS, Weickmann KM (2001) Sub seasonal variations of tropical convection and week-2 prediction of wintertime western North American rainfall. *J Clim* 14:3279–3288. [https://doi.org/10.1175/1520-0442\(2001\)014%3c3279:SVOTCA%3e2.0.CO;2](https://doi.org/10.1175/1520-0442(2001)014%3c3279:SVOTCA%3e2.0.CO;2)
- Wilson EA, Gordon AL, Kim D (2013) Observations of the Madden Julian oscillation during Indian Ocean dipole events. *J Geophys Res: Atmos* 118(6):2588–2599. <https://doi.org/10.1002/jgrd.50241>
- Wu J, Ren HL, Zuo J, Zhao C, Chen L, Li Q (2016) MJO prediction skill, predictability, and teleconnection impacts in the Beijing Climate center atmospheric general circulation model. *Dyn Atmos Oceans* 75:78–90. <https://doi.org/10.1016/j.dynatmoce.2016.06.001>
- Yesubabu V, Srinivas CV, Langodan S, Hoteit I (2016) Predicting extreme rainfall events over Jeddah, Saudi Arabia: impact of data assimilation with conventional and satellite observations. *QJR* 142(694):327–348. <https://doi.org/10.1002/qj.2654>
- Zhang C (2005) Madden-Julian oscillation. *Rev Geophys* 43:1–36. <https://doi.org/10.1029/2004RG000158>
- Zhang CD (2013) Madden-Julian oscillation bridging weather and climate. *Bul AMS* 94:1849–1870. <https://doi.org/10.1175/BAMS-D-12-00026.1>
- Zhao C, Li T, Zhou T (2013) Precursor signals and processes associated with MJO initiation over the tropical Indian Ocean. *J Clim* 26(1):291–307. <https://doi.org/10.1175/JCLI-D-12-00113.1>
- Zhao Y, Chen D, Li J, Chen D, Chang Y, Li J, Qin R (2020) Enhancement of the summer extreme precipitation over North China by interactions between moisture convergence and topographic settings. *Clim Dyn* 54(5):2713–2730. <https://doi.org/10.1007/s00382-020-05139-z>
- Zheng T, Feng T, Xu K, Cheng X (2020) Precipitation and the associated moist static energy budget off western Australia in conjunction with Ningaloo Niño. *Front Earth Sci* 8:597915. <https://doi.org/10.3389/feart.2020.597915>
- Zipser EJ, Cecil DJ, Liu C, Nesbitt SW, Yorty DP (2006) Where are the most intense thunderstorms on earth? *Bul AMS* 87:1057–1071. <https://doi.org/10.1175/BAMS-87-8-1057>